UW-Madison.
SSEC Publication No.96.08.S2.

Space Science and Engineering Center
University of Wisconsin–Madison

A REPORT
OF THE
UNIVERSITY OF WISCONSIN-CIMSS
SEVERE WEATHER PROGRAM
FOR THE PERIOD
1 SEPTEMBER 1995 TO 31 AUGUST 1996

A REPORT from the

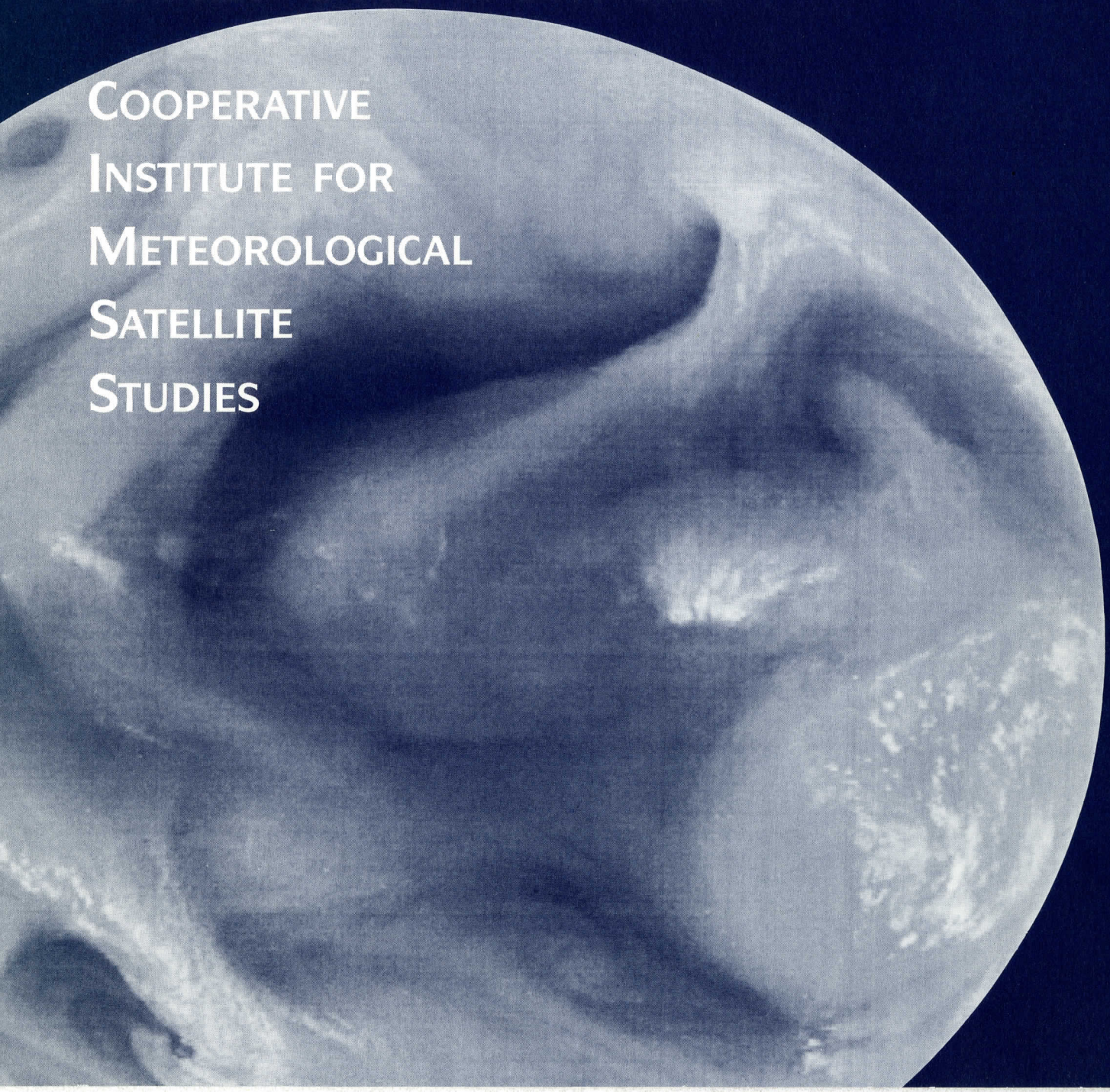

COOPERATIVE INSTITUTE FOR METEOROLOGICAL SATELLITE STUDIES

The Schwerdtfeger Library
1225 W. Dayton Street
Madison, WI 53706

A REPORT
OF THE
UNIVERSITY OF WISCONSIN-CIMSS
SEVERE WEATHER PROGRAM
FOR THE PERIOD
1 SEPTEMBER 1995 TO 31 AUGUST 1996

Submitted by

Cooperative Institute for Meteorological Satellite Studies
Space Science and Engineering Center (SSEC)
at the University of Wisconsin-Madison
1225 West Dayton Street
Madison, Wisconsin 53706
(608) 263-7435

Christopher M. Hayden
Chief, SDAB
Principal Scientist

William L. Smith
Director, CIMSS
Principal Investigator

Anthony J. Schreiner
Associate Researcher
Program Manager

TABLE OF CONTENTS

I. INTRODUCTION

This report describes the work done on Research Grant #NA47EC0420-01 during the period 1 September 1995 through 31 August 1996. The purpose of this report is to provide a summary of the various and diverse projects being supported during the contract period; results are provide in Section II. Sections III and IV summarize the scope of the research work and list references, respectively.

The primary objectives of this grant are twofold. The first objective is the use of remote sensing data to study the evolution of the storm environment. This includes investigations of the moisture budget and cloud conditions over meso to cyclone periods. The second objective is the examination of the dynamical and statistical evolution of the storm environment through use of remote sensing data assimilated into numerical weather prediction models. The program is thus directed at end-to-end application of satellite data to culminate in improved applications of satellite data to the severe weather forecasting problem.

The main research areas covered in Section II of this report are:

- The evolution of and improvements to the CIMSS Regional Assimilation System (CRAS) model. Continued streamlining and additional applications are being developed for the CRAS.
- The development of satellite-derived products using the VISSR Atmospheric Sounder (VAS) and the GOES-8 Sounder and Imager radiance information. Areas of concentration continue to be application of derived-products for the purpose of understanding and forecasting the weather, assimilation into numerical prediction models, and, through comparison to high spatial and temporal CLASS rawinsondes, verification of the remotely sensed temperature and moisture soundings.

II. RESULTS

A. Improved Precipitation Forecasts Using Parameterized Feedback in a Hydrostatic Forecast Model. Contributed by William H. Raymond and Robert M. Aune

An empirical Rayleigh drag parameterization of the non-hydrostatic mechanisms of precipitation drag and small-scale diabatically-induced mixing is introduced into a hydrostatic regional forecast model to curb excessive grid scale precipitation production. To get the necessary damping the coefficient in the Rayleigh drag is set proportional to the predicted liquid water, similar in form to the precipitation drag exhibited in non-hydrostatic calculations. The Rayleigh drag parameterization is found to be greatly superior to using the full non-hydrostatic precipitation drag term which produces a damping that is much too large in magnitude for use in a hydrostatic model. Even a re-scaling of this non-hydrostatic term is found to be unsatisfactory since it lacks the sensitivity required for hydrostatic calculations, resulting in an inability to control excessive precipitation.

To incorporate non-hydrostatic vertical acceleration effects into a hydrostatic model, we use a modified version of the quasi-hydrostatic approximation (Orlanski 1981). Two precipitation events are examined in detail while statistics for several other forecasts are also presented. Without the Rayleigh drag, excessive grid scale precipitation occurs. Two different cumulus parameterizations and three different turbulence schemes were unable to provide a satisfactory remedy for the excessive mesoscale precipitation. This study finds that the forecasted amount of precipitation depends strongly on the characteristics of the horizontal smoothing. Low order diffusion is found to restrict the mesoscale precipitation, but it also hampers the development of strong gradients and is highly non-conservative. This contrasts with a sixth order tangent filter which is more conservative and selective in controlling numerical noise while allowing sharper gradients and greater mesoscale development and precipitation. In our study, forecasts using the new Rayleigh drag parameterization are compared with actual precipitation observations. The new drag parameterization significantly reduces the excessive precipitation production while not impairing light precipitation.

In a study testing some of our modeling ideas, we produced synthetic water vapor (channel 12) brightness temperature fields from the model calculations for comparison with observed GOES water vapor images. This comparison helped us test different modeling techniques. A sample model representation of channel 12 brightness temperatures is illustrated in Figure 1. These were produced by using the forecast model fields in a forward radiative model which contains the appropriate GOES weighting functions.

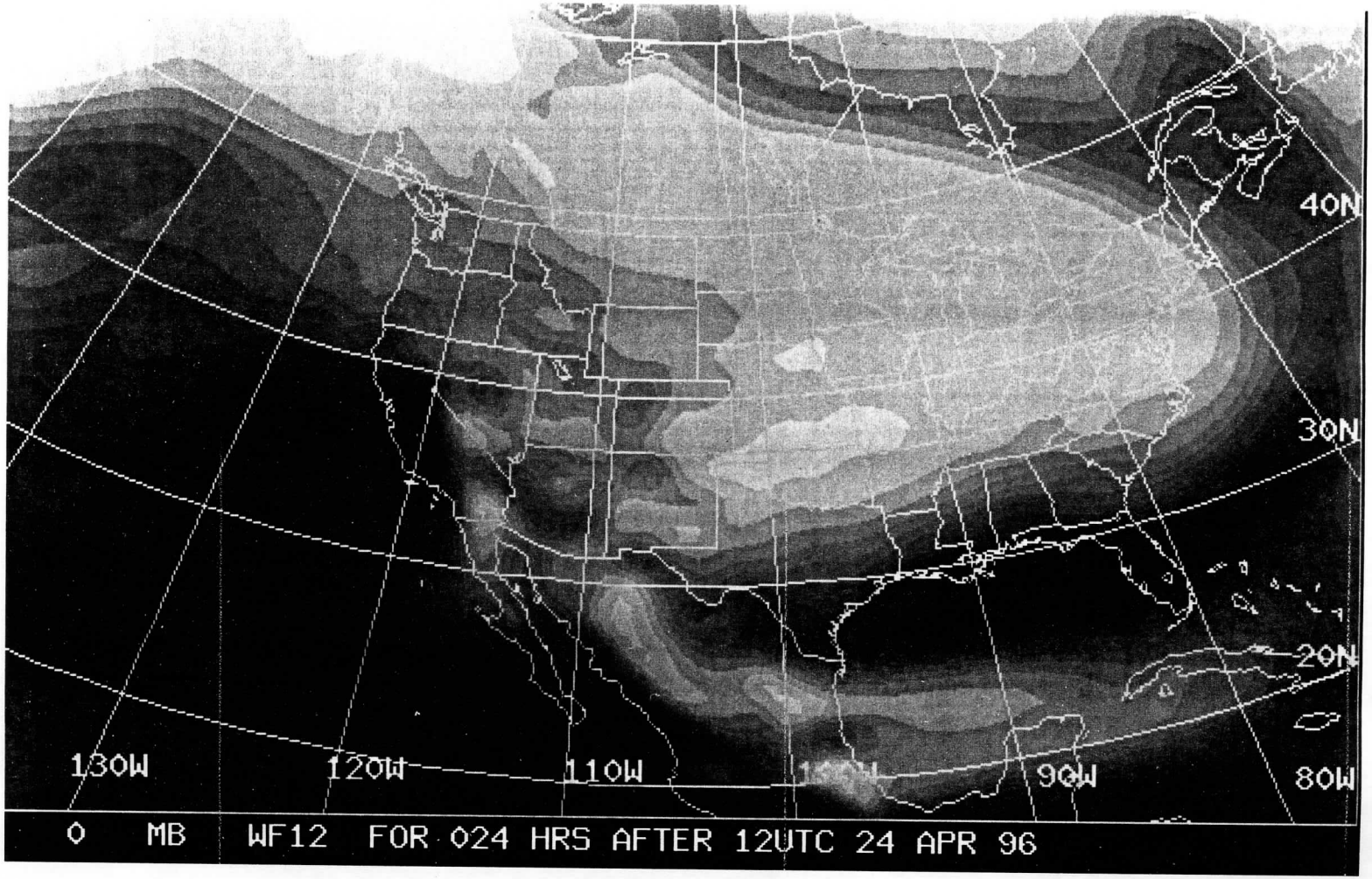

Figure 1 - A model representation of GOES channel 12 (6.5 micrometers)

B. A Theoretical Evaluation of the Relevance of Lognormal Distributions for the Moisture Flux and Moist Wind. Contributed by William H. Raymond

The lognormal distribution appears very commonly in rainfall and cloud statistics. This was first documented in detail by Biondini (1976) and Lopez (1977). A very large collection of literature in the atmospheric sciences now exists on this subject (e.g., Crane 1985, Kedem et al 1990). Nevertheless, the exact reason for the occurrence of this particular distribution has not been explained in terms of first principles. While turbulence, diffusion, or other physical properties of the atmosphere influence diabatic processes, the role of moisture flux and the supporting dynamics are also major influences. If the moisture flux satisfies the lognormal distribution, convective events, which need moisture to support their development, would likely be encouraged to adopt a similar distribution. In our study we show that the linear feedback to the moisture flux (dynamics) from diabatic processes is consistent with lognormal distributions.

It is reasonable to assume that moisture flux and moisture convergence are fundamental to and highly correlated with diabatic activity. The homogeneous equation for the inviscid vertical kinematic moisture flux wq is

$$d(wq)/dt = A(wq) + \dots \ , \tag{1}$$

where A=Q/q, where Q is negative when representing the mesoscale condensation rate and positive for the evaporation rate, while q is the mixing ratio. All other terms in the vertical flux equation are implicitly accounted for in the particular solution.

The solution of the homogeneous equation illustrated in (1) is

$$\ln(wq)_h=\ln(wq)_{t=0} + \int A \, dt. \tag{2}$$

The importance of this homogeneous solution depends upon the magnitude of A which contains the latent heating. If it is assumed that all samples of A belong to the same probability distribution function, one may claim with some confidence that ln(wq) asymptotically approaches a normal distribution (Aitchison and Brown, 1957). Consequently, $(wq)_h$ asymptotically approaches a lognormal distribution. This is true in both a Lagrangian and local (fixed) sense, since the latter requires only a linearization of the total derivative in (1). Thus, the lognormal behavior for the vertical moisture flux described above is the consequence of a

diabatic feedback mechanism. Similarly, it can be shown that all components of the moisture flux have solutions which behave in this manner. Consequently, all three components of the kinematic moisture flux are associated with homogeneous solutions that asymptotically approach distributions with lognormal properties. This statement is true for all atmospheric diabatic scales provided the ratios Q/q contained in the integrands all belong to the same probability distribution function.

While other studies have shown that stochastic approaches provide a viable explanation for lognormal distributions, they nevertheless must be considered secondary to solutions explicitly described by the inviscid governing equations, since, e.g., in our study it is shown that the equations for the kinematic moisture fluxes contain terms that yield homogeneous solutions with lognormal characteristics directly because of the interaction between diabatic processes and the flux components. This tendency to produce lognormal distributions is caused by a linear feedback mechanism that depends upon the strength of the diabatic process. This is consistent with the findings of Bell and Reid (1993) who identified that the larger rain rates are approximated better by the lognormal distribution.

Knowledge of the distribution of rainfall has helped in modeling and in the remote measuring of precipitation processes (Bell 1987). Similar knowledge about the diabatic contribution to the ageostrophic wind field and moisture flux should be useful in future remote sensing.

C. **Numerical Modeling/Data Assimilation at CIMSS.** Contributed by Robert M. Aune

The CIMSS modeling group continues to develop and test algorithms for assimilating data from the GOES-8/9 sounders. The CIMSS Regional Assimilation System (CRAS) has been used extensively to assess the data from GOES. Positive impact has been realized using retrievals of total precipitable water and cloud-top pressure from the GOES-8/9 sounders. In addition, multi-spectral, high-density winds from GOES have been used with good success. Operating in a "near real-time" mode allows CIMSS scientists to fully concentrate on data impact studies while monitoring CRAS model behavior. The current CRAS forecast system uses an 80 km grid nested within NMC's Aviation model. A 48-hour forecast is generated twice daily using data from the GOES-8/9 sounders. Control forecasts without GOES data, are generated when satellite data impact is suspect. Verification statistics are routinely compiled to assess the impact of the GOES data.

The modeling group at CIMSS conducted research in two areas. The first field of research examined GOES-8/9 assimilation potential. The quantification of information contained in radiance measurements from satellites is not new. Peckham (1974), Rodgers (1976), and more recently Eyre (1990) applied the concept of "information entropy" (Shannon, 1949) in their respective works on theoretical radiometer performance, temperature retrievals from measured radiances, and the information potential of TOVS/ATOVS. Purser and Huang (1993) used Bayesian statistical principles to objectively compute "effective data density" in satellite retrievals and analysis schemes. In this work the proposed method allows for the direct comparison of the information entropy of a background analysis with collocated multi-spectral radiance measurements from satellites. A value-added parameter is computed in the form of an entropy reduction, using computed error covariances of the model background and the instrument weighting functions. For the comparison, the method is extended to rawinsonde measurements by computing comparative "satellite-like" weighting functions for each rawinsonde valid at the analysis time and computing their respective entropies. This entropy reduction methodology was tested using the CRAS. The system provides a software platform for the development and testing of satellite data retrieval and assimilation algorithms.

The 80 km/29 level version of CRAS was used for this test. Background error covariances were computed using CRAS 12 hour forecasts verified against CRAS analyses. Different regions within the CRAS domain were investigated. Entropy reductions were then accumulated over a 12

hour period for comparison against synoptic rawinsondes. The methodology described above can be easily extended to other assimilation systems and can also be used to check the relative value of an observing system during each season and during different synoptic regimes. Further experimentation is needed to see if the methodology can be applied to 3D and 4D model domains. The potential exists for applications in the areas of adaptive or targeted observing systems and observation quality control.

The second area of modeling research is cloud initialization. Cloud top pressure derived from the GOES-8 and GOES-9 sounders is used to initialize cloud fields in the CRAS. To build a 3D cloud field using only cloud-top pressure observations requires the use of additional information to specify the depth of the cloud and the vertical distribution of the cloud water mixing ratio. The vertical profile of the water vapor mixing ratio, collocated with the cloud, may also need to be modified so that the model physics will support the existence or absence of a cloud. The technique is summarized as follows:

1. The observed cloud-top pressures are analyzed to the model grid (80 km). For this experiment a zero field first guess is used. Predicted cloud water fields from a previous forecast have also been used with good success.
2. Model grid points containing clouds are identified. An effective cloud emissivity fraction below 50% is considered clear. This threshold may vary with model resolution. The correlation between effective emissivity fraction, cloud depth and cloud height is currently under investigation.
3. A cloud base is computed by searching for dry layers below the cloud top. The updated (using rawinsonde dewpoints) model moisture analysis is used. If a suitable layer exists, a parabolic cloud water profile is computed following Wu et al. (1995). Maximum cloud depths are parameterized as a function of the cloud-top height. Vertical motions generated by the models vertical normal-mode initialization have been used to identify areas of active cloud production with good success. A 1D cloud model is currently being considered to initialize developing clouds in these areas.
4. The initial mixing ratio profile is adjusted to support the presence of cloud water. Since a specified relative humidity profile is used to control the growth and dissipation of cloud water in the model physics, the mixing ratio must be modified or the initialized clouds may quickly disappear.

Figure 1 shows an image of cloud-top pressures from the GOES-8 sounder valid at 0000 UTC on 1 September 1995. Figure 2 shows an IR image derived from the model atmosphere after the insertion of the GOES-8 cloud-top pressure retrievals from 0000 UTC 1 September 1995. It compares well with Figure 1. Implicit in the GOES-8 cloud data sets are clear sky observations. These are useful when assimilating cloud data in a 4D mode for controlling the over-production of

clouds and identifying deficiencies in a particular forecast. In addition, precipitable water retrievals are available from the same radiance data set over clear areas.

The impact of initializing the cloud water field is determined by comparing forecasts with initialized clouds (INCLD) to parallel forecasts with zero initial cloud water (NOCLD). Verification of 12 hour forecasted temperatures at 925 hPa, 850 hPa, and 700 hPa against rawinsonde temperatures consistently show a slight reduction in RMS and bias. Table 1 shows the verification statistics for a 12 hour temperature forecast valid at 1200 UTC on 1 September 1995. Although the improvement here is small, it is consistently positive from day to day.

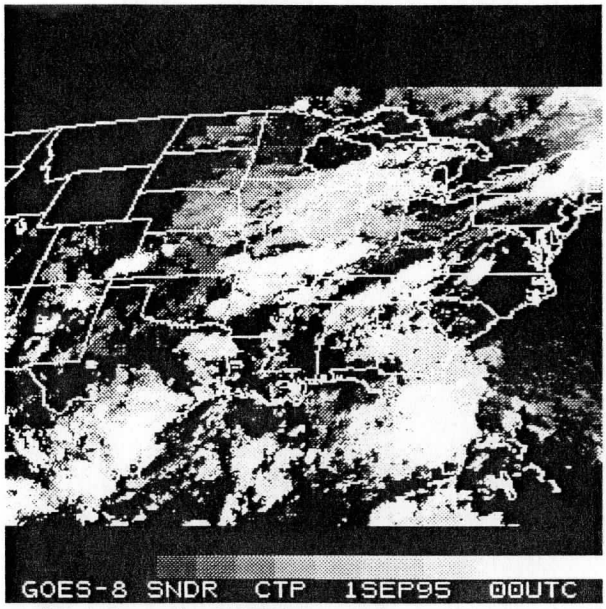

Fig 1. Cloud-top pressure (hPa) from the GOES-8 sounder valid 0000 UTC 1 September 1995. Gray scale ranges from dark (1000 hPa) to white (100 hPa).

Table 1. Verification statistics for a twelve hour temperature forecast valid at 1200 UTC on 1 September 1995.

TABLE 1

LEVEL	NOCLD	INCLD	NOCLD	INCLD
hPa	RMS	RMS	BIAS	BIAS
925 T	1.48	1.46	1.18	1.14
850 T	1.42	1.40	.88	.85
700 T	1.53	1.51	1.02	.99

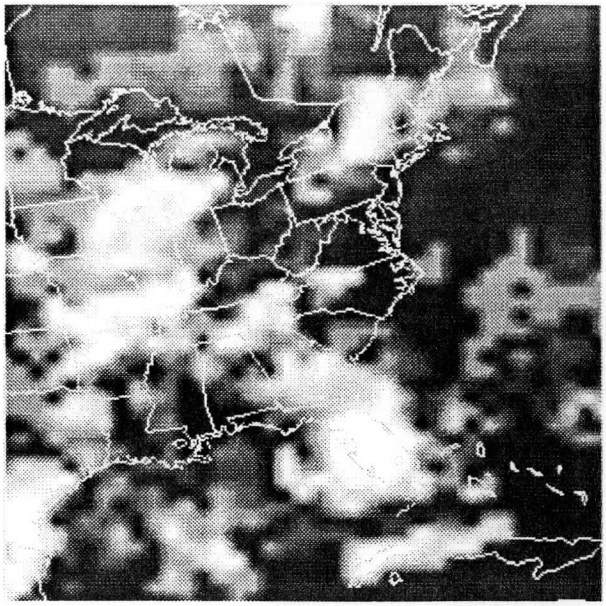

Fig 2. Derived IR image of cloud-top pressure (hPa) from CRAS initial fields after inserting GOES-8 sounder data valid 0000 UTC 1 September 1995. Gray scale range is similar to Fig 1.

New upgrades are frequently required to meet the objectives of CIMSS scientists who are interested in analyzing their data and looking at data impact. New upgrade features of the CRAS expected in the future include: enhanced physics, coupling of convective cloud to the grid-scale cloud physics, and non-local turbulence parameterization.

D. Estimating Water Vapor Profiles. Contributed by William H. Raymond

In this study simplified approximations for the vertical water vapor profile are derived from first principles. Surprisingly, the definition of the mixing ratio reduces to a power law or exponential power law approximation if the relative humidity is held constant. In our analytical derivation the exponents in the power law and exponential formulations are explicitly defined. It is found that the assumptions used in deriving the power law formulation only introduce a small loss of accuracy. For constant relative humidity this error varies approximately between 3 to 10% over vertical intervals having a temperature change of approximately 20 to 30 K. However, this error is tiny when compared to the inaccuracy introduced by assuming that the relative humidity remains constant over an extended interval. This assumption arises due to a lack of knowledge about a parcel's source region or from not knowing its recent vertical transport history, both of which influence the relative humidity. A large part of the missing information involves the modification of the relative humidity by compressional warming or expansional cooling. These effects are included in this study along with a free parameter e which can be used to constrain the relative humidity (mixing ratio) to satisfy the precipitable water or an observed relative humidity. This information acts as a proxy for the historical information which is otherwise missing. Remote sensing is capable of providing this type of information. Including compressional and expansional effects greatly improves the ability of the power law approximation to estimate the vertical water vapor profile.

Figures 1 and 2 illustrate the rms. and bias errors for the power law approximation, between 925 and 511 hPa. These calculations use T0 and q0 from the 925 hPa level in a zero time-step CRAS (CIMSS Regional Assimilation System) forecast which uses a smoothed NCEP (National Center for Environmental Prediction) initialized data set for 1200 UTC 18 April 1996 to obtain the initial meteorological fields. The horizontal grid is composed of 73 x 53 points of 150 km resolution while the vertical coordinate contains 20 sigma levels. This April case has relatively cool temperatures in the northern part of the domain while very warm temperatures dominate in its southern latitudes.

In the control calculations (e=0) shown in Figures 1 and 2, the relative humidity does not vary over the vertical interval 925 - 511 hPa. In this study, to compensate for a lack of information about the relative humidity profile, a free parameter (e) in the compressional term is tuned either by knowledge of the precipitable water (Epsilon Pw) or by knowledge of the relative humidity at the top of the interval (Epsilon Rh). Nearly an order of magnitude improvement is obtained in the rms. and bias errors in Figures 1 and 2 by including the constraints. Without the constraints the bias error in Figure 2 greatly over-estimates the mixing ratio. This is because upper level moisture usually contains less humidity than that observed at 925

hPa where T0 and q0 are set. The results from our experiment are clear. Estimating the mixing ratio without allowing for variations in the relative humidity leads to large errors in the moisture profile. Some of this error can be removed provided one knows an additional piece of information, like the precipitable water or the relative humidity at an isolated point. In our study we show that the power law approximation for the mixing ratio, with constraints applied to the compressional factor, produces rms and bias errors that are the same order of magnitude as realized for idealized (constructed) moisture profiles having a constant relative humidity. Compared with previous work (Smith, 1966), our description of the power law, with compressional effects included, allows for a more physically meaningful evolution of the moisture profile because relative humidity variations are included.

List of Figures

Figure 1 - Root mean square errors of the total precipitable water profile (g./kg) using the power law approximation between 925 and 511 hPa based on the 1200 UTC 18 April 1996 initialized data set.

Figure 2 - Same as Figure 1 except bias errors are depicted.

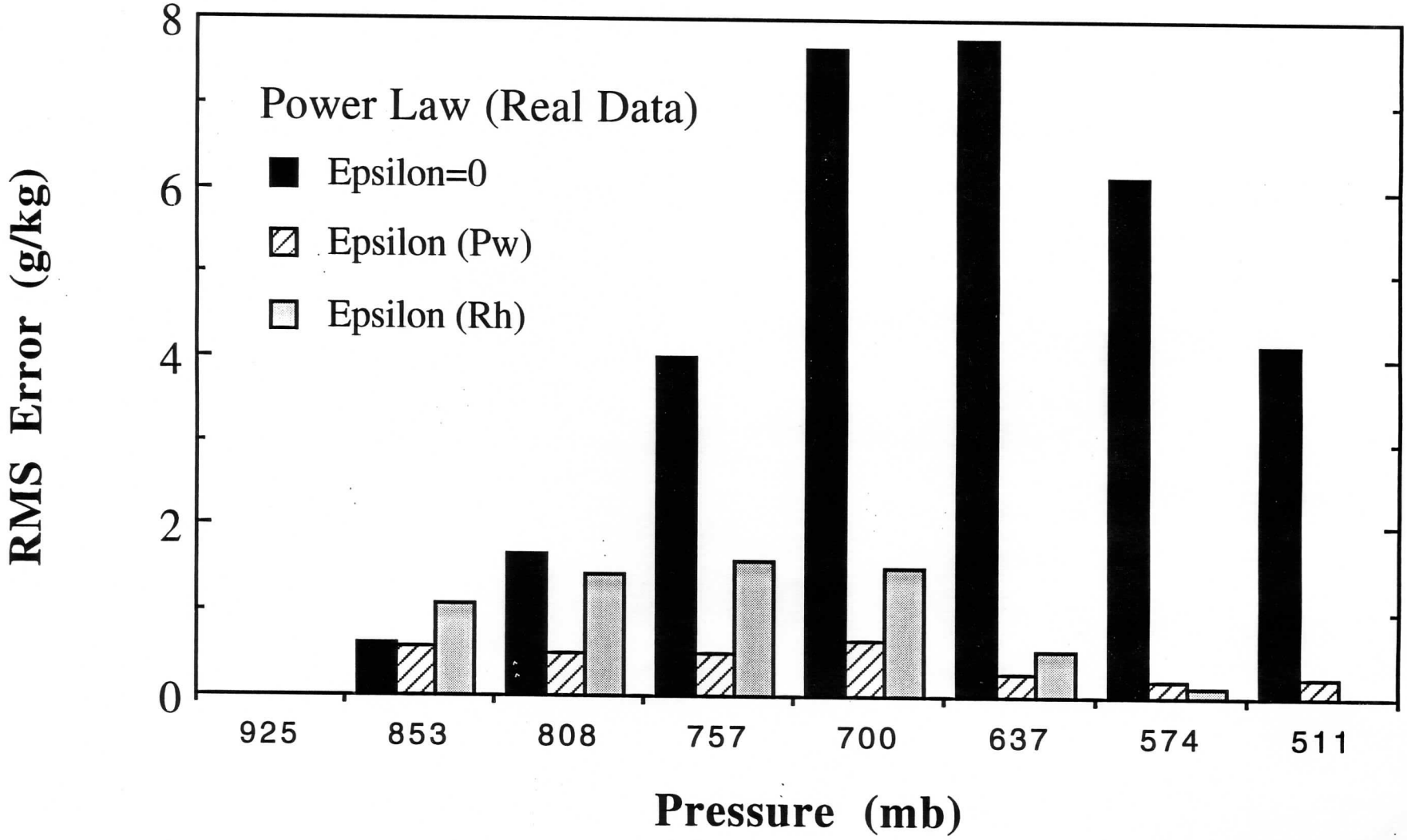

Figure 1 - Root mean square errors of the total precipitable water profile (g/kg) using the power law approximation between 925 and 511 hPa based on the 1200 UTC 18 April 1996 initialized data set.

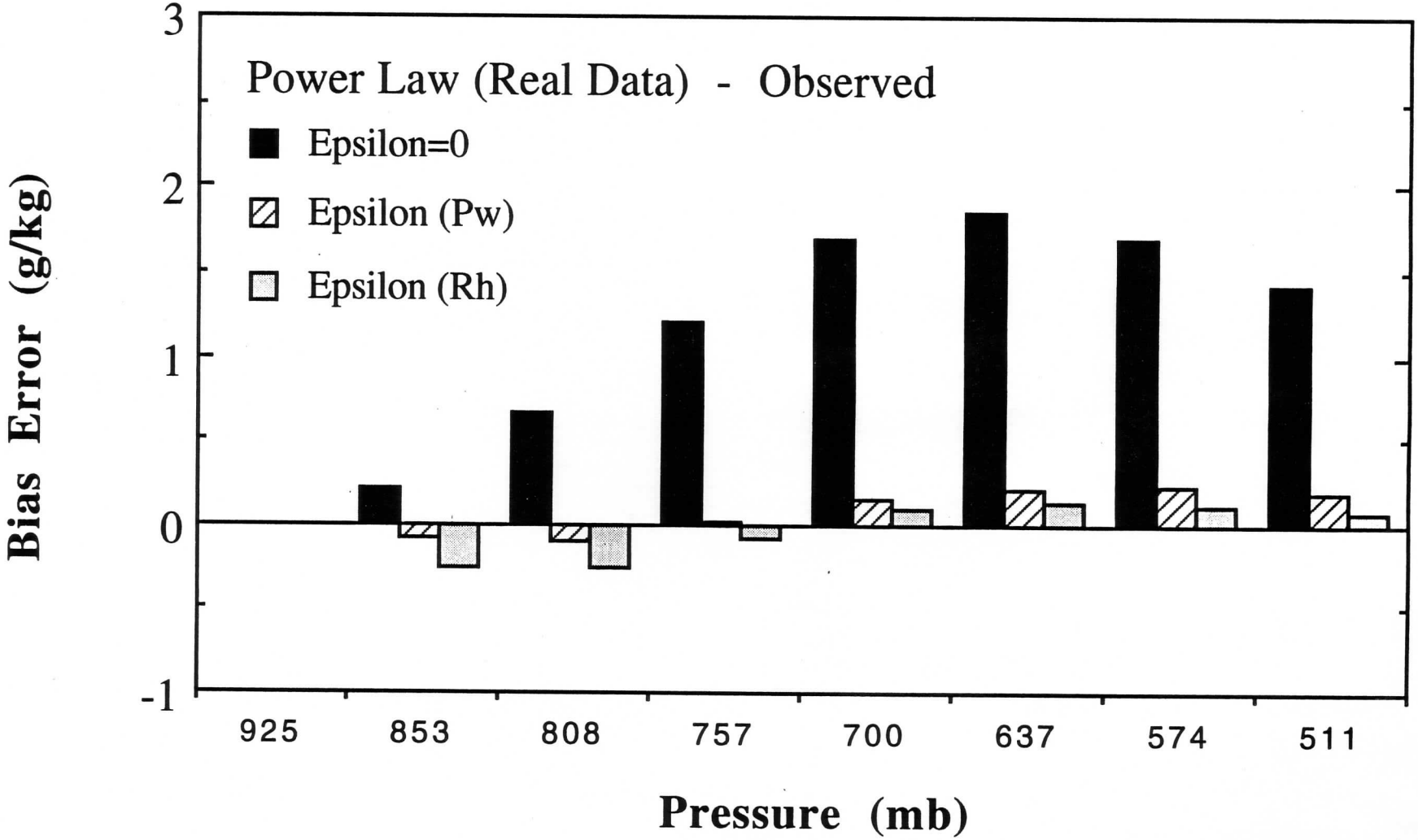

Figure 2 - Same as Figure 1 except bias errors are depicted.

E. Application of GOES-8 Sounder data to Mesoscale Analysis. Contributed by Robert M Rabin (visiting scientist, NSSL), Tim Schmit and Gary Wade.

The GOES sounder data has been tested in diagnosing hourly changes in atmospheric stability and moisture in the vicinity of convergence zones and developing thunderstorms over land. A detailed analysis has been undertaken for a data set during the Verification of Tornadoes Experiment (VORTEX) on 22 May 1995 where scattered storms developed in the vicinity and ahead of a strong dry line in the Texas panhandle and Oklahoma.

Using 6-12 hour forecasts from the Nested Grid Model (NGM) and hourly synoptic surface data as a first guess, retrieved profiles of temperature and moisture were derived from the hourly GOES-8 sounder radiances. Retrievals were processed with varying resolutions of 30x30 km and 50x50 km for comparison with VORTEX mesoscale soundings (Hayden and Schmit, 1994; Hayden and Schmit, 1995). In addition, single field of view (10x10km) estimates of precipitable water (PW) and lifted index were made using a non-linear physical retrieval algorithm developed by Ma et al. (1996).

As an example, first guess and derived images of PW and lifted index are shown in Figures 1 and 2 for 2100 UTC on 22 May 1995. The numbers overplotted on the images are from the 30x30 km retrievals (small font), and derived from rawinsondes (large font). Clouds are shown as gray and white with the brightness proportional to their height. The west to east gradient in PW across the dry line is evident in both the guess and retrieved images. However, the use of the GOES data intensifies the gradient and produces values closer to those deduced from several of the rawinsondes. The difference is generally within 2-3 mm. Near strong gradients, the 30x30 km retrievals compare better with the rawinsondes than 50x50 km products do (not shown). The retrievals also detect bands of increased PW feeding into the convective storms from the south. These features do not appear in the guess fields. The wide band of high PW to the east of the dry line is obscured in its center by stratus cloud, which is indicated by gray in the figures. The impact of the satellite data is also to intensify the east to west gradient in lifted index along the dry line. The most unstable air is in a narrow band just ahead of the dry line, to the west of the highest moisture. Initial storm development in the eastern Texas panhandle is along this band, downwind of the most unstable region. A time series of these images indicates eastward progression of these features and an increase in moisture content ahead of the growing storm. These results were presented at the Fifth National Heavy Precipitation Workshop sponsored by the NWS, State College, PA, 9-13 September 1996.

List of Figures

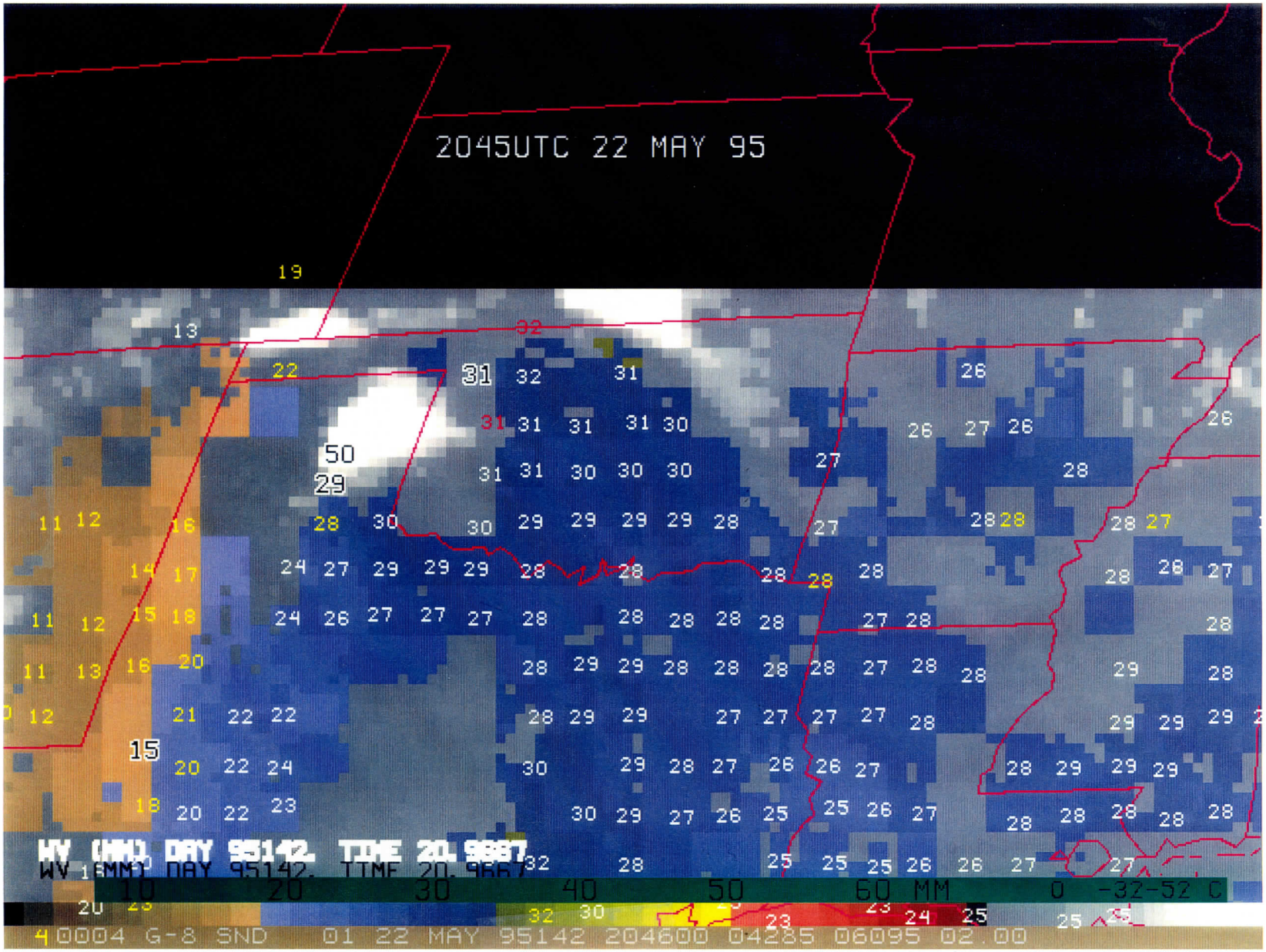

Figure 1a - Total precipitalbe water for 21UTC 22 May 1995. Large font values are derived from rawinsondes and small font values are retrieved from the first guess.

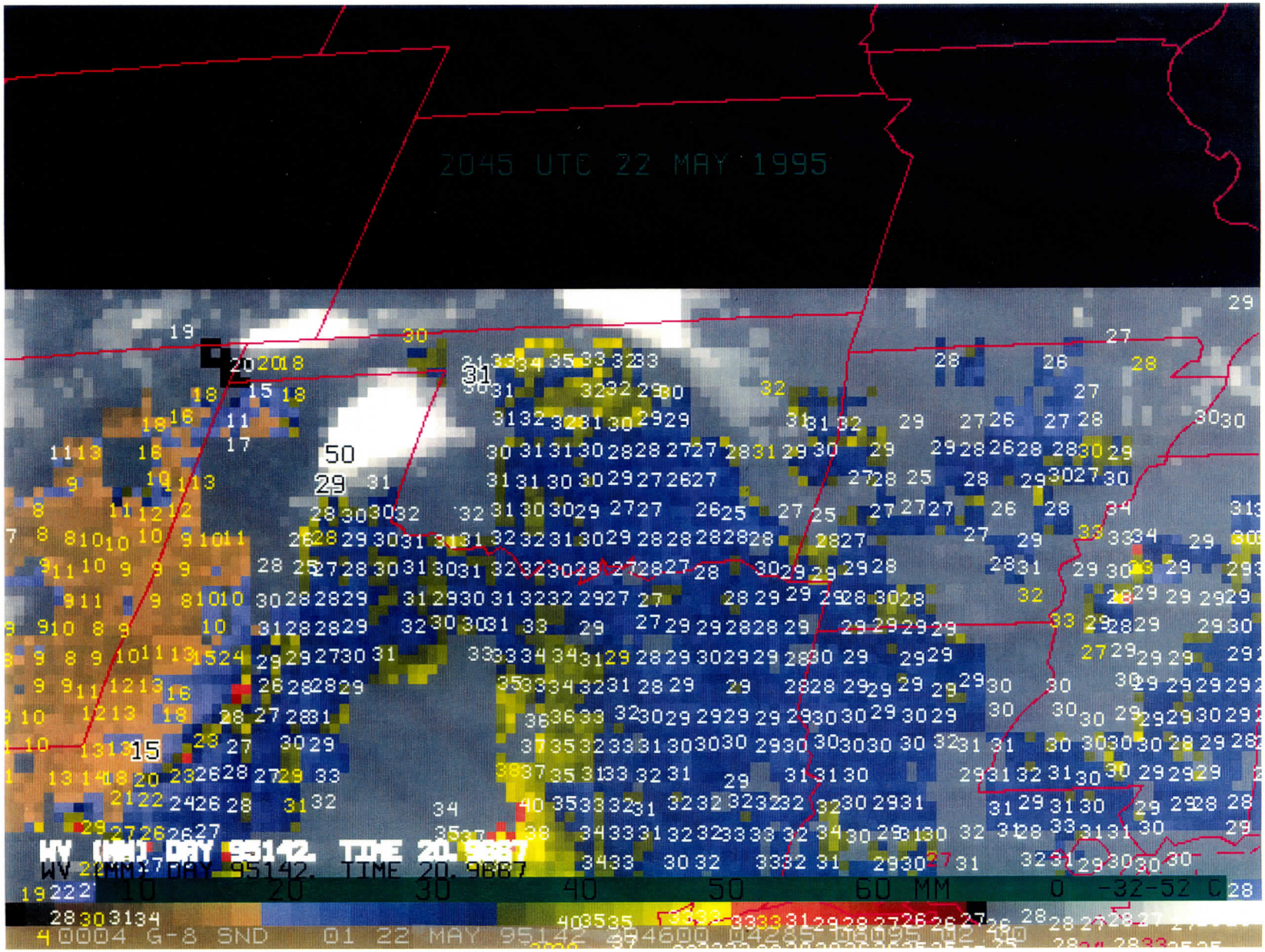

Figure 1b - Same as Figure 1a, except the small font values are derived from GOES-8 sounder radiance data.

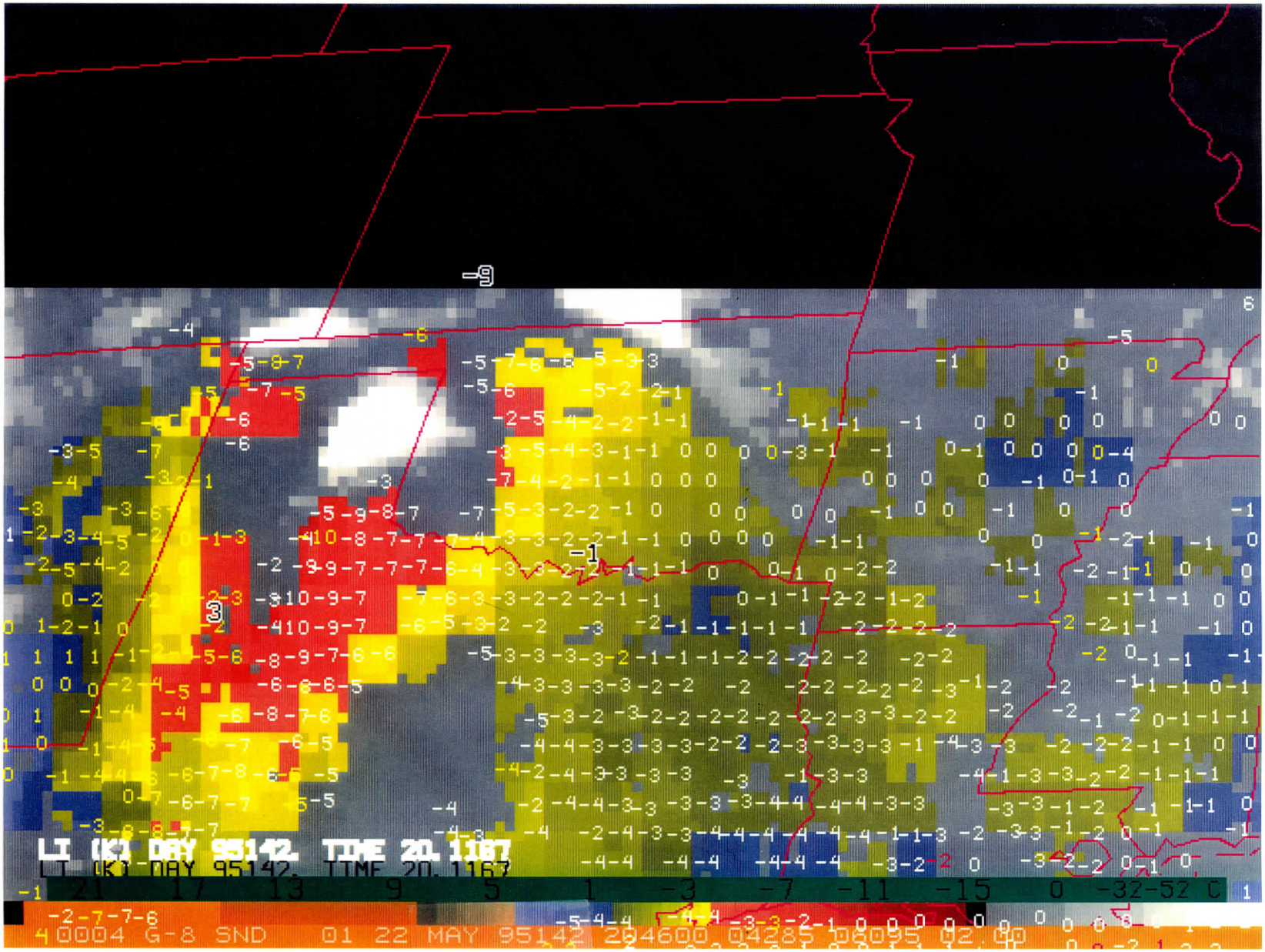

Figure 2a - Same as Figure 1a, except derived information is lifted index.

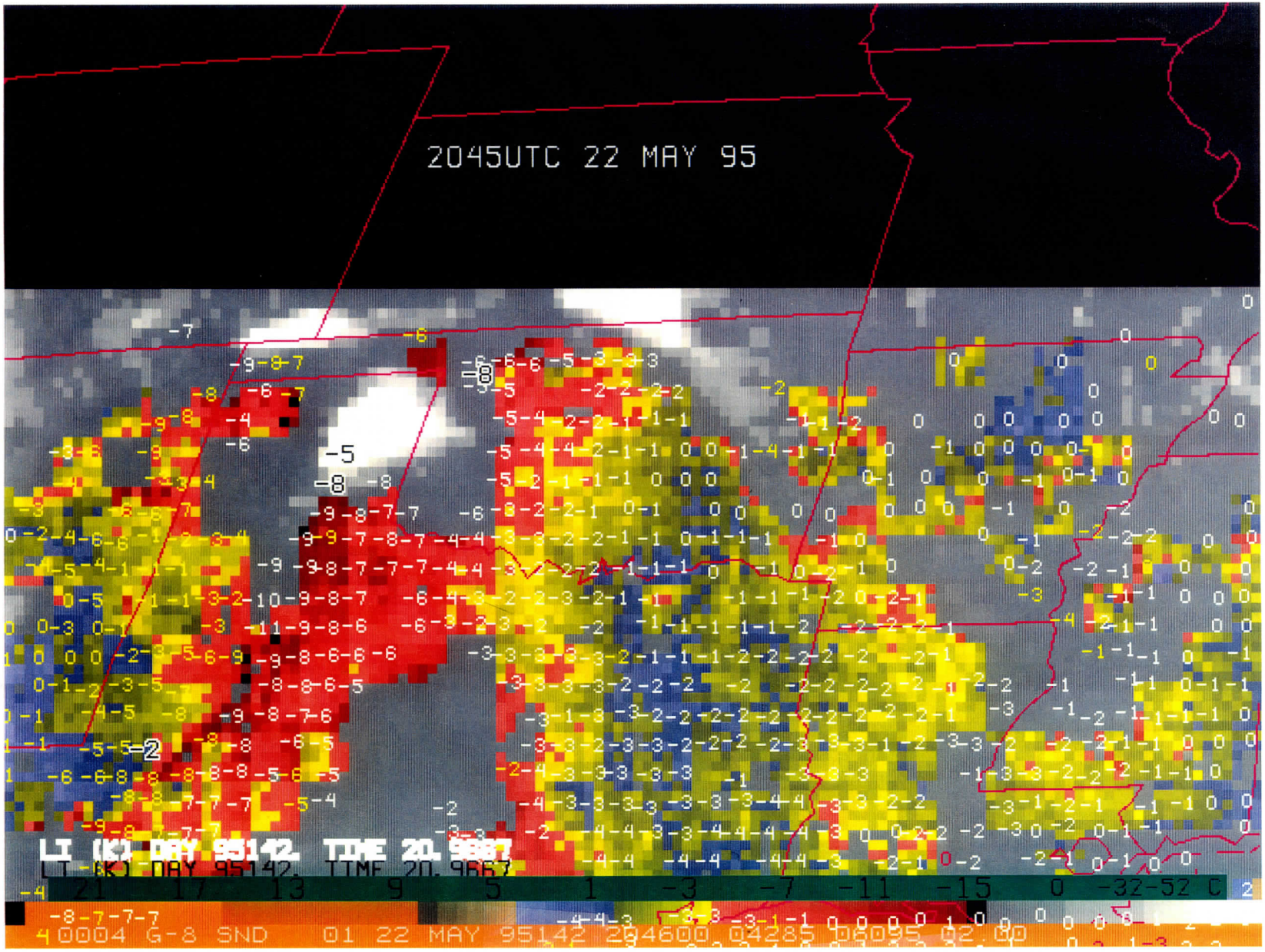

Figure 2b - Same as Figure 1b, except derived information is lifted index.

III. SUMMARY

Over the past year this grant has been a primary source and impetus for the continued development and assimilation of satellite-derived products into numerical weather prediction models. An example of this evolutionary process is the effort being directed toward initializing forecast models with atmospheric moisture and cloud parameters derived from remotely sensed radiance data. It has been demonstrated that this information can be routinely calculated from the latest version of GOES. Techniques for incorporating this information into prediction models have been developed and shown to improve forecasts on both a coarse and fine scale.

Support through this contract is important to provide CIMSS researchers the opportunity to perform a wide variety of numerical weather prediction investigations. These studies are a first step toward a more complete application of remotely sensed products in the weather forecasting problem.

IV. REFERENCES

Orlanski, I., 1981: *The quasi-hydrostatic approximation. J. Atmos. Sci.*, **38**, 572-582

Hayden, C.M. and T. J. Schmit, 1994: GOES-I Temperature Moisture Retrievals and Associated Gradient Wind Estimates. 7th conference on Satellite Met. and Ocean. June 6-10. Monterey, CA., 385-398.

Hayden, C.M. and T. J. Schmit, 1995: Initial Evaluation of the GOES-8 Sounder 9th conference on Met. Observ. and Instr. March 27-31. Charlotte, NC., 477-480.

Ma, Xia L., W. L. Smith, T. J. Schmit, 1996: A non-linear physical retrieval algorithm-Its application to the GOES-8/9 Sounder. Submitted to *J. Appl. Meteor.*

Eyre, J. R., 1990: The information content of data from satellite sounding systems. *Q. J. R. Meteorol. Soc.*, **116**, 401-434.

Peckham, G., 1974: The information content of remote measurements of the atmospheric temperature by satellite IR radiometry and optimal radiometer configurations. *Q. J. R. Meteorol. Soc.*, **100**, 406-419.

Purser, R. J. and H.-L. Huang, 1993: Estimating effective data density in a satellite retrieval or an objective analysis. *J. Appl. Meteor.*, **32**, 1092-1107.

Rodgers, C. D., 1976: Retrieval of atmospheric temperature and composition from remote measurements of thermal radiation. *Rev Geophys.Space Phys.*, **14**, 609-924.

Shannon, C., 1949: Communication in the presence of noise. *Proc I.C.E.*, **37**, 10-21

Wu, X., G. R. Diak, C. M. Hayden, 1995: Short-range precipitation forecasts using assimilation of simulated satellite water vapor profiles and column cloud liquid water amounts. *Mon. Wea. Rev.*, **123**, 347-365.

Aitchison, J., and J. A. C. Brown, 1957: *The lognormal distribution.* Cambridge University Press, 176pp.

Bell, T. L., 1987: A space-time stochastic model of rainfall for satellite remote-sensing studies. *J. Geophys. Res.*, **92**, 9631-9643.

Bell, T. L., and N. Reid, 1993: Detecting the diurnal cycle of rainfall using satellite observations. *J. Appl. Meteor.*, **32**, 311-322.

Biondini, R., 1976: Cloud motion and rainfall statistics. *J. Appl. Meteor.*, **15**, 205-224.

Crane, R. K., 1985: Evaluation of global and CCIR models for estimation of rain rate statistics. *Radio Sci.*, **20**, 865-879

Kedem, B., L. S. Chiu, and G. R. North, 1990: Estimation of mean rain rate: Application to satellite observations. *J. Geophys. Res.*, **95D**, 1965-1972.

Lopez, R. E., 1977: The lognormal distribution and cumulus cloud populations. *Mon. Wea. Rev.*, **105**, 865-872.

Smith, W.L., 1966: Note on the relationship between total precipitable water and surface dew point. *J. Appl. Meteor.*, **5**, 726-727.